

Nonlinear Adaptive Sliding-Mode Control Design for Two-Wheeled Human Transportation Vehicle

Shui-Chun Lin, *Member, IEEE*,
 Department of Electronic
 Engineering, National Chin-Yi
 University of Technology,
 Taichung 41101, Taiwan, R. O. C.
 email:lsc@ncut.edu.tw

Ching-Chih Tsai*, *Senior Member, IEEE*,
 Department of Electrical Engineering,
 National Chung-Hsing University,
 Taichung 40027, Taiwan, R. O. C.
 email:cctsai@nchu.edu.tw

Hsu-Chih Huang, *Member, IEEE*,
 Department of Computer Science and
 Information Engineering,
 HungKuang University,
 Taichung, Taiwan, R. O. C.
 email:hchuang@sunrise.hk.edu.tw

Abstract—This paper presents adaptive sliding-mode control methods for self-balancing and yaw rate control of a dynamically two-wheeled human transportation vehicle (HTV) with mass variations and system uncertainties. The proposed controllers aim to provide consistent driving performance for system uncertainties and different drivers whose weights cause parameter variations of the HTV. By decomposing the overall system into the yaw subsystems and the self-balancing subsystems with parameters variations with respect to different riders, two adaptive sliding mode controls are proposed to achieve self-balancing and yaw control. Numerical simulations and experimental results on different terrains show that the proposed adaptive sliding mode controllers are capable of achieving satisfactory control actions to steer the vehicle.

Keywords—adaptive control, gyroscope, inverted pendulum, robotics transporter, sliding mode control.

I. INTRODUCTION

Recently, self-balancing two-wheeled transporters, like the Segway™, have been well recognized as powerful personal transportation vehicles. The kind of transporter can be usually constructed by a synthesis of mechatronics, control techniques and software. For example, the Segway™ is made by quite high-tech and high-quality dedicated components. In contrast to the Segway™, many researchers [1]-[2] presented low-tech self-balancing transporters and claimed that the vehicle can be built using the off-the-shelf inexpensive components. With the advent of modern technology, such transporters with sophisticated safety features can be cost down so that they, like traditional bicycles, have high potential to become prevalent two-wheeled HTVs, satisfying human transportation requirements.

Design and implementation of a safe and practical self-balancing HTV is a very interesting problem. Grasser *et al.* [1] built a scaled down prototype of a digital-signal-processor (DSP) controlled two wheeled vehicle based on the inverted pendulum with weights attached to it, and Pathak *et al.* [3] studied the dynamic equations of the wheeled inverted pendulum by partial feedback linearization. However, they are test prototypes, aiming at providing several theoretical design and analytical approaches. Furthermore, several researchers in [4]-[8] proposed useful control and implementation techniques for four-wheeled vehicles, two-wheeled vehicles with differential driving, and electric scooter. However, these methods can not be directly applied to address both self-balancing and yaw control problems for the two-wheeled self-balancing HTV.

Recently, sliding mode control (SMC) have been adopted widely for nonlinear system modeling and control because they possess simple structure, good local approximating performance, particular resolvability, and function equivalence to a simplified class of nonlinear systems. Many successful applications on fuzzy control were reported in various areas; for example, Nawawi *et al* [10] proposed the modeling of 2-wheels Inverted Pendulum and the design of proportional integral sliding-mode control (PISM) for the system., Yu *et al* [11] presented a variable structure control (VSC) algorithm to achieve the prespecified trajectory tracking on mechatronic arms. Lam *et al* [12] proposed two adaptive fuzzy controllers are used to control the inverted pendulum to track a given position and balance the pole.

The paper contributes to the design of two adaptive sliding-mode controllers for achieving self-balancing and yaw control. Like the JOE in [1], the proposed controllers are synthesized by decoupling this vehicle system into two subsystems: yaw motion and mobile inverted pendulum. In comparison with the state-feedback design presented by Grasser *et al.* [1], the key features of the proposed control method hinge on its nonlinear mathematical modeling with coulomb and static frictions, and its adaptive control for the HTV with unknown plant parameters, unknown frictions and linearized errors. Moreover, the proposed controllers are useful in keeping consistent driving performance for different riders.

The rest of the paper is outlined as follows. Section II briefly describes the system design of the vehicle and Section III shows the synthesis procedures of the two adaptive controllers using sliding-mode control. In Section IV computer simulations and experimental results are presented and discussed. Section V concludes the paper.

II. SYSTEM DESCRIPTION AND MODELING

A. Control Architecture

Fig.1 depicts the free body diagram of the HTV, and Fig.2 illustrates the block diagram of the HTV control system. The DSP controller with built-in A/D conversion is responsible for executing both adaptive yaw motion and self-balancing control algorithms. The pitch rate ω_p from the gyroscope and the pitch angle θ_p from the tilt sensor are utilized via the controllers to maintain the human body on the footplate without falling. Note that both feedback signals are processed

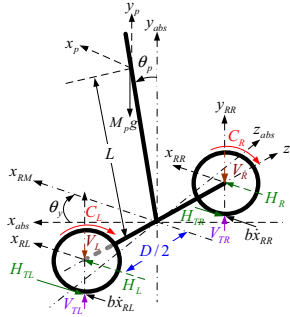


Fig. 1. Free body diagram of the HTVs.

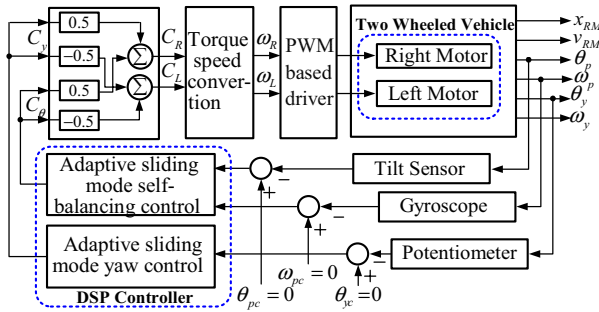


Fig. 2. Block diagram of the HTV controller.

by two first-order filters, thus removing unwanted noise. The potentiometer is adopted to measure the yaw angle from the handlebar, and the yaw signal is then taken by the DSP controller for further yaw control. The output torque commands from the DSP controller are converted into the corresponding speed commands via a torque-to-speed formula.

B. Mathematical Modeling

To obtain high-performance steering experience for different riders, it is necessary to develop a mathematical model of the vehicle. The nonlinear mathematical model of the HTV with both frictions is modified from [1] and given in the following state equation

$$\begin{bmatrix} \dot{x}_{RM} \\ \dot{v}_{RM} \\ \dot{\theta}_p \\ \dot{\omega}_p \\ \dot{\theta}_y \\ \dot{\omega}_y \end{bmatrix} = \begin{bmatrix} v_{RM} \\ A_{22}v_{RM} + A_{23}\sin\theta_p \\ \omega_p \\ A_{43}\sin\theta_p \\ \omega_y \\ A_{66}\omega_y \end{bmatrix} + \begin{bmatrix} 0 & 0 \\ B_2 & B_2 \\ 0 & 0 \\ B_4 & B_4 \\ 0 & 0 \\ B_6 & -B_6 \end{bmatrix} \begin{bmatrix} C_L \\ C_R \end{bmatrix} + \begin{bmatrix} 0 \\ f_2 \\ 0 \\ f_4 \\ 0 \\ f_6 \end{bmatrix} \quad (1)$$

where x_{RM} [m] and v_{RM} [m/s] respectively denote the position and velocity of the HTV respect to the world frame; θ_p [rad] and ω_p [rad/s] respectively represent the pitch angle and pitch angle rate of the HTV; θ_y [rad] and ω_y [rad/s] respectively stand for the yaw angle and yaw rate of the HTV; C_L [N-m] and C_R [N-m] respectively denote the applied torques on the left and right wheels; f_i ($i = 2, 4, 6$) respectively denotes the

uncertain term which may include coulomb and static frictions, and linearized errors. Similar to the vehicle, called JOE, developed by Grasser *et al.*[1], the following decoupling transformation from C_θ and C_y into the wheel torques C_R and C_L is used to decouple the system model such that both yaw motion and inverted pendulum controllers are independently designed.

$$C_L = 0.5(C_\theta + C_y), \quad C_R = 0.5(C_\theta - C_y) \quad (2)$$

which converts the system (1) into two subsystems; one is the mobile inverted pendulum subsystem described by

$$\begin{bmatrix} \dot{\theta}_p \\ \dot{\omega}_p \end{bmatrix} = \begin{bmatrix} \omega_p \\ A_{43}\sin\theta_p \end{bmatrix} + \begin{bmatrix} 0 \\ B_4 \end{bmatrix}(C_\theta + \bar{f}_4), \quad \bar{f}_4 = f_4 / B_4 \quad (3)$$

and the other is the yaw control subsystem described by

$$\begin{bmatrix} \dot{\theta}_y \\ \dot{\omega}_y \end{bmatrix} = \begin{bmatrix} 0 & 1 \\ 0 & A_{66} \end{bmatrix} \begin{bmatrix} \theta_y \\ \omega_y \end{bmatrix} + \begin{bmatrix} 0 \\ B_6 \end{bmatrix}(C_y + \bar{f}_6), \quad \bar{f}_6 = f_6 / B_6 \quad (4)$$

Note that the model for the uncertainties, f_2 , f_4 and f_6 can be realistically modeled by

$$f_2 = B_{23}f_{dRL} + B_{24}f_{dRR} + B_{25}f_{dp}$$

$$f_4 = B_{45}f_{dp}$$

$$f_6 = B_{63}f_{dRL} + B_{64}f_{dRR}$$

where f_{dRL} , f_{dRR} and f_{dp} are three disturbance forces exerted on the left wheel, the right wheel, and the handle-bar, respectively.

$B_{23} = B_{24} = \frac{R^2}{2J_R\alpha}$, $B_{25} = \frac{R^2}{2J_R}\frac{1}{\alpha\beta}\cdot\frac{J_{p\theta}}{M_pL\cos\theta_p}$, $B_{45} = \frac{1}{\beta M_p}$, $B_{63} = -B_{64} = D/\left[2pJ_{py}\right]$, where $\alpha = [M_RR^2/J_R] + 1$, $\beta = [J_{p\theta}/M_pL\cos\theta_p] + L\cos\theta_p$ and R is radius of the wheels, J_R is moment of inertia of the wheel, $J_{p\theta}$ is moment of inertia of the chassis with respect to the z axis, M_p is mass of the chassis with the weight of the rider, L is distance between the z axis and the center of gravity of the chassis, θ_p is pitch angle, D is lateral distance between the contact patches of the wheels, J_{py} is moment of inertia of the chassis with respect to the y axis, $p = 1 + [D^2(J_R + M_RR^2)/2J_{py}R^2]$, and M_R is mass of the wheel.

III. CONTROLLER DESIGN

A. Nonlinear Sliding-mode Self-Balancing Control Design

This subsection will consider constructing an adaptive sliding-mode self-balancing controller for the subsystem (3) where A_{43} and B_4 are known, but the nonlinear term \bar{f}_4 is unknown. A block diagram of the control system for the transporter is shown in Fig.2. The control objective is to control the angle position θ_p to reach to the command position θ_{pc} without error under the aforementioned settings. Due to the nonlinearity of system mode (3), the well-known sliding mode technique is adopted to accomplish the control

goal. To maintain the angle position θ_p at $\theta_{pc} = 0$, one recalls the nonlinear subsystem model of the human transporter:

$$\begin{aligned}\dot{\theta}_p &= \omega_p \\ \dot{\omega}_p &= A_{43} \sin \theta_p + f_4 + B_4 C_\theta\end{aligned}\quad (5)$$

To achieve self-balancing of the transporter, one defines the sliding surface by

$$s = K_1 \theta_p + \omega_p, K_1 > 0 \quad (6)$$

Let $G = (K_1 \omega_p + A_{43} \sin \theta_p + f_4) / B_4$ and the uncertainty satisfies the following inequality

$$|G| \leq \delta(\theta_p, \omega_p) \quad (7)$$

To stabilize the system (5), we propose the following torque control:

$$C_\theta = \beta(\theta_p, \omega_p) \operatorname{sgn}(s), \beta(\theta_p, \omega_p) > \delta(\theta_p, \omega_p) \quad (8)$$

To show that θ_p will tend to zero as time approaches infinity, the following Lyapunov function is chosen by

$$V_1 = s^2 / 2 \quad (9)$$

Then the time derivative of the Lyapunov function V_1 becomes

$$\begin{aligned}\dot{V}_1 &= s \dot{s} = s \left[A_{43} \sin \theta_p + B_4 (C_\theta + \bar{f}_4) + K_1 \omega_p \right] \\ &= s B_4 [C_\theta + G]\end{aligned}\quad (10)$$

Substituting (8) into (10) leads to

$$\dot{V}_1 = s B_4 [\beta(\theta_p, \omega_p) \operatorname{sgn}(s) + \delta(\theta_p, \omega_p)]$$

Using the inequality (7) and the subsequent inequality

$$s [\beta(\theta_p, \omega_p) \operatorname{sgn}(s) + \delta(\theta_p, \omega_p)] \geq [(\beta(\theta_p, \omega_p) - \delta(\theta_p, \omega_p)) |s|] \geq 0$$

One obtains

$$\dot{V}_1 = B_4 [(\beta(\theta_p, \omega_p) - \delta(\theta_p, \omega_p)) |s|] \leq 0 \quad (11)$$

Since \dot{V}_1 is semi negative-definite, the Lyapunov stability theory implies $s \rightarrow 0$ as $t \rightarrow \infty$. On the sliding surface $s = 0 = K_1 \theta_p + \omega_p = K_1 \theta_p + \dot{\theta}_p$, it is easy to show that $\theta_p \rightarrow 0$ as $t \rightarrow \infty$.

Theorem 1 Consider the subsystem (5) with the proposed control (8). Then the pitch will remain at $\theta_{pc} = 0$ as $t \rightarrow \infty$.

B. Nonlinear Adaptive Sliding-mode Self-Balancing Control Design

Due to difficulty to estimate $\delta(x)$ in practice, it is rather difficult to implement the proposed self-balancing control law (8). To circumvent the shortcoming, this subsection will pay effort to design a new kind of adaptive robust self-balancing control law so that the transporter can be maintained in the desired operating range of the pitch angle. In doing so, suppose that $\delta(x)$ is bounded, i.e.,

$$|G| \leq \delta(\theta_p, \omega_p) \leq \delta_{\max} \quad (12)$$

To stabilize the system (5), the following torque control is proposed by

$$C_\theta = (\beta_0 + \hat{\delta}) \operatorname{sgn}(s), \beta_0 > 0 \quad (13)$$

where $\hat{\delta}$ is to be estimated such that θ_p will tend to zero as time approaches infinity. This can be easily proven by choosing the following Lyapunov function

$$V_2 = (s^2 / 2) + (\hat{\delta}^2 / 2\lambda) B_{4(\min)} \quad (14)$$

where $B_{4(\min)} / \lambda > 0$ and $B_{4(\min)} \leq B_4 < 0$ over the desired operating range of the pitch angle. Therefore, the time derivative of the Lyapunov function V_2 is found by

$$\begin{aligned}\dot{V}_2 &= s \dot{s} + \frac{B_{4(\min)}}{\lambda} \dot{\hat{\delta}} \tilde{\delta} = s(K_1 \dot{\theta}_p + \dot{\omega}_p) + \frac{B_{4(\min)}}{\lambda} \dot{\hat{\delta}} \tilde{\delta} \\ &= B_{4(\min)} \left\{ s [C_\theta + G] + \tilde{\delta} (-\dot{\hat{\delta}}) / \lambda \right\}\end{aligned}\quad (15)$$

where $\tilde{\delta} = \delta_{\max} - \hat{\delta}$. If the adaptive parameter law is selected by

$$\dot{\hat{\delta}} = \lambda |s|, \lambda < 0 \quad (16)$$

$$\begin{aligned}\text{then } \dot{V}_2 &\leq s \dot{s} + \frac{B_{4(\min)}}{\lambda} \dot{\hat{\delta}} \tilde{\delta} \leq B_{4(\min)} \tilde{\delta} |s| + \frac{B_{4(\min)}}{\lambda} \tilde{\delta} [-\dot{\hat{\delta}}] + B_{4(\min)} \beta_0 |s| \\ &= B_{4(\min)} \beta_0 |s| \leq 0\end{aligned}\quad (17)$$

From (17), the Lyapunov stability theory and the comparison lemma implies $s \rightarrow 0$ as $t \rightarrow \infty$.

Theorem 2 Consider the subsystem (5) with the proposed adaptive robust control (13) and the parameter adjustment law (16). Then the angle position θ_p will be maintained at $\theta_{pc} = 0$, i.e., $\theta_p \rightarrow 0$ as $t \rightarrow \infty$.

C. Nonlinear Sliding-mode Yaw Control Design

This subsection will consider constructing an adaptive sliding-mode self-balancing controller for the subsystem (4) where A_{66} and B_6 are known, but the nonlinear term \bar{f}_6 is unknown. A block diagram of the control system for the transporter is shown in Fig.2. Since the potentiometer is employed to measure the angle difference between the equilibrium point and the yaw angle the rider intended to achieve, the adaptive yaw control problem is reduced to an adaptive regulation problem. Therefore, the backstepping technique is used to attain the sliding-mode yaw controller by choosing the virtual control $\omega_y = -K_y \theta_y$ and the Lyapunov function $V_3 = \theta_y^2 / 2$, and then stabilizing the θ_y -dynamics. Next, define the second backstepping error

$$\xi_y = \omega_y - \phi(y_e) = \omega_y - \phi(y_e) = \omega_y + K_y \theta_{ye} = \dot{\theta}_{ye} + K_y \theta_{ye} \quad (18)$$

Differentiating ξ_y gives

$$\begin{aligned}\dot{\xi}_y &= \dot{\omega}_y + K_y \dot{\theta}_y = [A_{66} \omega_y + B_6 (C_y + \bar{f}_6)] + K_y \omega_y \\ &= B_6 \left[\left(\frac{K_y + A_{66}}{B_6} \right) \omega_y + (C_y + \bar{f}_6) \right]\end{aligned}\quad (19)$$

In order to stabilize the yaw control subsystem, we will consider the sliding surface

$$s = \eta = \omega_y + K_y \theta_{ye} \quad (20)$$

Differentiating s gives

$$\dot{s} = \dot{\eta} = B_6 \left\{ \left[(K_y + A_{66}) / B_6 \right] \omega_y + (C_y + \bar{f}_6) \right\} \quad (21)$$

where $K_y + A_{66} > 0$, $\left| \frac{K_y + A_{66}}{B_6} \right| < K_1$, $\bar{f}_6 < K_0$

To stabilize the system (4), we propose the following torque control:

$$C_y = (-K_1 \omega_y - K_0) \operatorname{sgn}(s) \quad (22)$$

The following Lyapunov function candidate is chose by $V_3 = s^2 / 2$

Differentiating the Lyapunov function V_3 yields

$$\begin{aligned} \dot{V}_3 &= ss = B_6 \left\{ s \left(\frac{K_y + A_{66}}{B_6} \omega_y \right) + s \bar{f}_6 - \left[(K_1 |\omega_y| + K_0) |s| \right] \right\} \\ &\leq B_6 \left\{ |s| \left(\left| \frac{K_y + A_{66}}{B_6} \right| |\omega_y| \right) + |s| \bar{f}_6 - \left[(K_1 |\omega_y| + K_0) |s| \right] \right\} \\ &= B_6 \left\{ - \left[K_1 - \left| \frac{K_y + A_{66}}{B_6} \right| \right] |\omega_y| - (K_0 - |\bar{f}_6|) |s| \right\} < 0 \end{aligned} \quad (23)$$

Since \dot{V}_3 is semi negative-definite, the use of the comparison lemma implies $s \rightarrow 0$ as $t \rightarrow \infty$. On the sliding surface $s = 0 = \omega_y + K_y \theta_y$, it is easy to show that $\theta_y \rightarrow 0$ as $t \rightarrow \infty$.

Theorem 3 Consider the subsystem (4) with the proposed control (22). Then the pitch will remain at $\theta_{pc} = 0$ as $t \rightarrow \infty$

D. Nonlinear Adaptive Sliding-mode Yaw Control Design

This subsection is devoted to constructing an adaptive sliding-mode yaw controller for the subsystem (4) with the two parameters, A_{66} and B_6 , and the unknown nonlinear term \bar{f}_6 . Since the potentiometer is employed to measure the angle difference between the equilibrium point and the yaw angle the rider intended to achieve, the adaptive yaw control problem is reduced to an adaptive regulation problem. Therefore, similar to the previous subsection, the backstepping technique is again used to attain the adaptive yaw controller by choosing the virtual control $\omega_y = -K_y \theta_y$ and the Lyapunov function $V_3 = s^2 / 2$, and then stabilizing the θ_y -dynamics.

Next, define the second backstepping error

$$\xi_y = \omega_y - \phi(y) = \omega_y + K_y \theta_y = \dot{\theta}_y + K_y \theta_y \quad (24)$$

Differentiating ξ_y gives

$$\begin{aligned} \dot{\xi}_y &= \dot{\omega}_y + K_y \dot{\theta}_y = \left[A_{66} \omega_y + B_6 (C_y + \bar{f}_6) \right] + K_y \omega_y \\ &= (K_y + A_{66}) \omega_y + B_6 (C_y + \bar{f}_6) \\ &= B_6 \left[\left(\frac{K_y + A_{66}}{B_6} \right) \omega_y + (C_y + \bar{f}_6) \right] \end{aligned} \quad (25)$$

In order to stabilize the yaw control subsystem, the implicit

control C_y with estimated parameters \hat{K}_1 and \hat{K}_0 is proposed as follows; for $K_2 > 0$ and $K_y > 0$,

$$C_y = (-\hat{K}_1 |\omega_y| - \hat{K}_0) \operatorname{sgn}(s) - K_2, \quad K_2 > 0 \quad (26)$$

The estimated parameters, \hat{K}_1 and \hat{K}_0 are defined by $\tilde{K}_0 = K_0 - \hat{K}_0$ and $\tilde{K}_1 = K_1 - \hat{K}_1$ differentiating the two equations to get $\dot{\tilde{K}}_0 = -\dot{\hat{K}}_0$ and $\dot{\tilde{K}}_1 = -\dot{\hat{K}}_1$. The following Lyapunov function candidate is employed to find the parameter updating laws

$$V_4 = \frac{1}{2} s^2 + \frac{B_6}{2\lambda_0} \tilde{K}_0^2 + \frac{B_6}{2\lambda_1} \tilde{K}_1^2 \quad (27)$$

Where $\lambda_0 > 0$, $\lambda_1 > 0$. Differentiating the Lyapunov function V_4 yields

$$\begin{aligned} \dot{V}_4 &\leq -K_{yp} K_y \theta_y^2 + \tilde{A}_{66} (\omega_y \xi_y - \dot{\hat{A}}_{66} / r_{ay}) \\ &\quad + \tilde{B}_6 [(-K_{yp} \xi_y \theta_y - \hat{A}_{66} \omega_y \xi_y - K_y \omega_y \xi_y) / \hat{B}_6 - \dot{\hat{B}}_6 / r_{by}] \\ &\quad + B_6 [\tilde{U}^T (S_y |\xi_y| - \dot{\hat{U}} / r_{ay})] + B_6 \dot{\xi}_y (|\xi_y| - \dot{\hat{\xi}}_y / r_{ey}) \end{aligned} \quad (28)$$

If the following parameter adaptation rules are chosen by

$$\begin{aligned} \dot{\hat{K}}_1 &= \lambda_1 |\omega_y| |s| \\ \dot{\hat{K}}_0 &= \lambda_0 |s| \end{aligned} \quad (29)$$

Then \dot{V}_4 becomes $\dot{V}_4 = -B_6 K_2 |s| \leq 0$ which implies $\theta_y \rightarrow 0$ as $t \rightarrow \infty$. The following summarizes the result.

Theorem 4 Consider the subsystem (4) with the proposed adaptive sliding-mode yaw control (26) with the parameter updating laws (29). Then $\theta_y \rightarrow \theta_{yc} = 0$, as $t \rightarrow \infty$.

IV. SIMULATIONS, EXPERIMENTAL RESULTS AND DISCUSSION

A. Mechatronic Design

Fig.3 displays the photographs of the laboratory-based personal two-wheeled HTV with differential driving. This vehicle is composed of one footplate, two 24V DC motors with a gearbox of ratio 20:1, two stamped steel wheels with 16-inch tires, two 12-volt sealed rechargeable lead-acid batteries in series, two motor drivers, a single chip DSP-TMS320LF2407 from Texas Instruments as a main controller, one handle-bar with a potentiometer as a position sensor, one gyroscope and one tilt sensor. The two motor drivers use dual H-bridge circuitry to deliver PWM-based power to drive the two DC servomotors. Sending PWM signals to the drives, the DSP outputs control signals, ranging from 0 V and 3.3 V_{DC}, to achieve self-balancing and yaw motion of the HTV. The gyroscope and the tilt sensor are employed for measuring the rate and the angle of the inclination of the footplate caused by the rider. The two rechargeable lead-acid batteries directly provide power for the two DC servomotors, drives, the controller and all the sensors via DC-DC buck conversion.

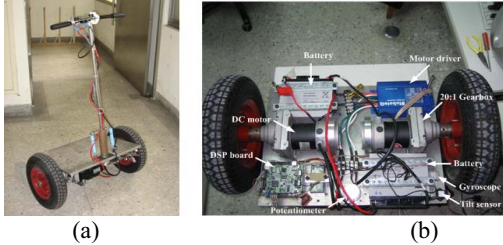


Fig.3. Laboratory-built personal two-wheeled HTV: (a) Front view (no human stand on it). (b) Bottom view.

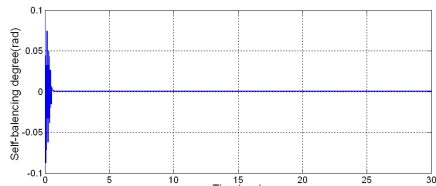


Fig.4. Simulation result of the self-balancing tracking

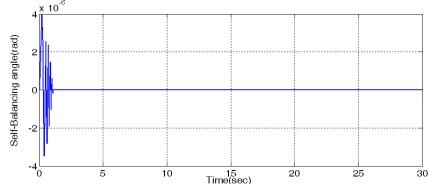


Fig.5. Sliding mode control with self-balancing angle.

B. Adaptive Sliding-mode Self-Balancing Control

This section is devoted to describing simulation results of the proposed adaptive Sliding-mode self-balancing control method. The relevant parameters used for the simulation are: $\theta_{com} = 0.025 \text{ rad}$, $K_p = 655$, $K_1 = 50$, $r_b = 0.0001$, $r_w = 0.001$, $r_a = 0.0001$. The control signal is limited to the output interval between -512 and 512. Figs.4 and 5 show the angle response of the inverted pendulum subsystem, indicating that the angle approached the desired angle about at 0.9 seconds.

C. Adaptive Sliding-mode Yaw Control

This subsection will conduct several simulations to examine the effectiveness of the proposed nonlinear sliding-mode yaw control. The relevant parameters used for simulations are: $\theta_{com} = 0.000001 \text{ rad}$, $K_1 = 10000$, $\beta_0 = 0.01$, $\lambda = -0.001$. Fig.6 presents the sliding surface of the controlled yaw angle subsystem. Fig.7 presents the simulation results of the yaw angles with initial errors of ± 0.2 rads. Clearly, the yaw angle tends to zero after 0.4 seconds.

D. Experimental Results and Discussion

The objective of the experiments is to examine the performance of the proposed sliding mode control laws for

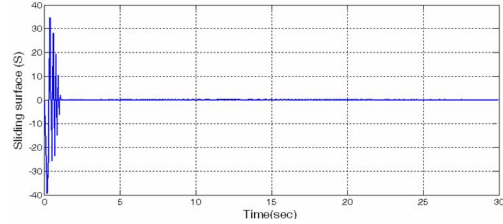


Fig.6. Sliding surface of the yaw angle subsystem.

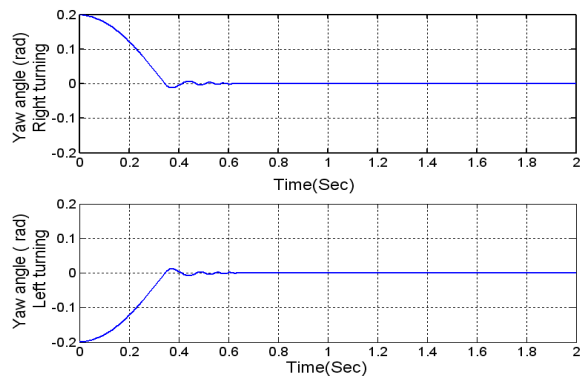


Fig.7. Simulation results of the yaw angle tracking.



Fig.7. The HTV ridden by students on a smooth floor. (a) Moving forward. (b) Moving backward.



Fig.8. The HTV moving on (a) Turning right. (b) Turning right.



(a)



(b)

Fig.9. The HTV moving on ramp terrains. (b) Going uphill.(c) Going downhill.

achieving self-balancing and yaw rate control. The performance of these controllers for the HTV is evaluated on three different experimental scenarios: moving on uneven terrains, turning right/left and moving forward/ backward.

1) Experimental results of the proposed self-balancing controllers

The real-time control codes of the proposed sliding mode self-balancing controllers were implemented by standard C language. Fig.7 shows the HTV ridden by students while the vehicle was moving forwards and backwards on the smooth floor. Assume that the HTV is operated near the origin condition, and the tilt error $e_\theta(t)$ is very small, but the derivative of the tilt error $e_\theta(t)$ can be large, and can be positive or negative, depending the operation condition. This large derivative requires a significant control effort to achieve self-balancing in the neighborhood of the origin.

2) Experimental results of the proposed yaw controllers

Two experiments were conducted to verify the performance of the designed sliding mode controllers. In order to perform the experiments, the sampled data transformations of the two controllers were obtained using the backward difference and bilinear transform methods, and the resultant digital control laws were coded by standard C language. Fig. 8 shows the HTV ridden by students while it was turning right and left.

3) Experimental results of the HTV on three different terrains

The performance of the HTV was investigated with a human rider on three different scenarios: smooth floor, uneven road and ramp terrain. Three experiments were conducted with the sliding mode self-balancing controller and the yaw controller. The HTV was safely steered on the smooth floor and a student comfortably rode the HTV on the uneven and ramp terrains, as shown in Fig.9. The human riding experience suggested that riding on the smooth floor be much easier than on the uneven or ramp terrain. It is worthwhile mentioning that when the HTV went uphill on the uneven or ramp terrain, the rider required a large tilt angle, but needed a small tilt angle for going downhill. This result is attributed to the fact that the centre of gravity of the HTV is vertical to the flat ground, but not to the ramp terrain.

V. CONCLUSIONS

This paper has presented adaptive sliding mode control method for self-balancing and yaw control of a two-wheeled self-balancing HTV driven by two DC servomotors. The mechatronic method has been used to construct the vehicle, including a differential driving mechanism, a control architecture using digital signal. The nonlinear mathematical modeling of the vehicle has been well established in a state-space framework. By decomposing the system into two subsystems: yaw and inverted pendulum, two adaptive sliding mode controllers have been synthesized to achieve self-balancing control and yaw control of the vehicle. Through simulation and experimental results, the proposed controllers have been shown useful and effective in providing appropriate control actions to steer the vehicle. An interesting topic for future work would be to apply a hierarchical decoupling sliding-mode controller to achieve self-balancing and speed control of this kind of human transportation vehicle.

ACKNOWLEDGEMENTS

The authors gratefully acknowledge financial support from the National Science Council, Taiwan, R.O.C., under grant contract NSC96-2218-E-005-045-MY2.

REFERENCES

- [1] F. Grasser, A. D. Arrigo, and S. Colombi, "JOE: A mobile, inverted pendulum," *IEEE Trans. Ind. Electron.*, vol. 49, no. 1, pp. 107-114, Feb. 2002.
- [2] S. C. Lin, C. C. Tsai, and W. L. Luo, "Adaptive neural network control of a self-balancing two-wheeled scooter," *In proc. 33rd Annu. IEEE IECON*. pp. 868-873, Nov. 5-8, 2007.
- [3] K. Pathak, J. Franch, and S. K. Agrawal, "Velocity and position control of a wheeled inverted pendulum by partial feedback linearization," *IEEE Trans. Robot. Autom.*, vol. 21, no. 3, pp. 505-513, Jun. 2005.
- [4] P. K. W. Abeygunawardhana and T. Murakami, "An Adaptive Based Approach to Improve the Stability of Two Wheel Mobile Manipulator," *In proc. 33rd Annu. IEEE IECON*. pp.2712 – 2717, 5-8, Nov.
- [5] H. Ohara and T. Murakami, "A stability control by active angle control of front-wheel in a vehicle system," *IEEE Trans. Ind. Electron.* vol. 55, no. 3, pp. 1277-1285, Mar. 2008.
- [6] I. Baturone, F. J. Moreno-Velo, V. Blanco, and J. Ferruz, "Design of embedded DSP-based fuzzy controllers for autonomous mobile robots," *IEEE Trans. Ind. Electron.*, vol. 55, no. 2, pp. 928-936, Feb. 2008.
- [7] C. H. Chen; M. Y. Cheng "Implementation of a highly reliable hybrid electric scooter drive," *IEEE Trans. Ind. Electron.*, vol. 54, no. 5, pp. 2462-2473, Oct. 2007.
- [8] N. Mutoh, Y. Hayano; H .Yahagi, and K. Takita, "Electric braking control methods for electric vehicles with independently driven front and rear wheels," *IEEE Trans. Ind. Electron.* vol. 54, no. 2, pp. 1168-1176, Apr. 2007.
- [9] H. K. Khalil, "Nonlinear Systems," 3rd Ed., Upper Saddle River, Prentice Hall, 2002.
- [10] S. W. Nawawi, M. N. Ahmad, J. H. S. Osman, A. R. Husain and M. F. Abdollah, "Controller Design for Two-wheels Inverted Pendulum Mobile Robot Using PISM," *In proc. 4th Student Conference on Research and Development.*, Shah Alam, Selangor, MALAYSIA, pp.194-199, 27-28 Jun.2006.
- [11] W. S. Yu and Y. H. Chen, "Decoupled Variable Structure Control Design for Trajectory Tracking on Mechatronic Arms" *IEEE Trans. Control Systems Technology*, vol. 13, no.5, pp.798-806, Sep.2005
- [12] Xiaojun, X. Z. Gao, and Xianlin, "Design of a hybrid fuzzy-PD controller for inverted pendulum," *In proc. 2004 IEEE International Conference on Systems, Man and Cybernetics*, pp. 2286 – 2291, vol.3, 10-13 Oct.2004.